American Mineralogist, Volume 65, pages 349–352, 1980

A neutron diffraction study of a one-layer triclinic chlorite (penninite)

WERNER JOSWIG, HARTMUT FUESS, RICHARD ROTHBAUER

Institut für Kristallographie und Mineralogie
Senckenberganlage 30, D-6000 Frankfurt am Main, Federal Republic of Germany

YOSHIO TAKÉUCHI

Mineralogical Institute, Faculty of Science
University of Tokyo, Hongo, Tokyo 113, Japan

AND SAX A. MASON

Institute Laue-Langevin
156 X F 38042 Grenoble-Cedex, France

Abstract

The crystal structure of a one-layer triclinic chlorite (penninite) was refined from three-dimensional neutron diffraction data. The structure shows the II*b*-4 stacking type with the cell constants: $a = 5.3266(7)$, $b = 9.232(1)$, $c = 14.399(3)$A, $\alpha = 90°$, $\beta = 97.16(1)°$, $\gamma = 90°$. The refinement, including site occupancies of tetrahedral and octahedral positions, gave a final $R(F) = 0.024$ for space group $C\bar{1}$. No cation ordering was detected in the talc sheets; cation ordering is, however, significant in the brucite sheets. The hydrogen-bonding system with respect to the stability of the different polytypes is discussed.

Introduction

The chlorites are a mineral group with layered structure. One layer is built up of alternating talc-like and brucite-like sheets. The crystal structure of a triclinic polymorph was first solved by Steinfink (1958). The mode of stacking sequences of the layers along the z direction gives rise to polytypes (one-, two-, three- *etc.* layer structures). Within the one-layer polytypes a differentiation was proposed by Bailey and Brown (1962). Their scheme is based on the various permissible ways to arrange the brucite sheet upon the talc sheet and on the superposition of the next talc sheet on the brucite sheet, resulting in 12 unique polytypes of the one-layer structure. In most chlorites a considerable degree of randomness has been observed, as indicated by diffuse streaks in precession photographs along $k \neq 3n$ row lines. The relative abundances of the polytypes have been discussed in terms of the cation repulsion and cation–anion attraction (Shirozu and Bailey, 1965). Since, however, the nature of the hydrogen-bonded systems in chlorite, which are thought to be essential in stabilizing the structure, is unknown, we have undertaken this neutron diffraction study.

Experimental

A large number of chlorite grains from a crystal druse—described as ripidolite from Zillertal, Tirol—were checked under a polarizing microscope and by the precession method to obtain a well-crystallized chlorite of suitable size for neutron diffraction work. A well-crystallized specimen ($k \neq 3n$ reflections showed no diffuseness) of the dimensions $2.0 \times 1.0 \times 0.5$ mm was chosen for the data collection. Because of the pseudohexagonal symmetry, the three possible y axes had to be tested to assure the y axis which is perpendicular to x and z. Among the possible polytypes only I*a*-4, II*a*-3, II*b*-4, and I*b*-4 (nomenclature of Bailey and Brown, 1952; Brown and Bailey, 1963) are in agreement with the symmetry of the precession photographs, which indicate space group $C\bar{1}$ or $C1$ with the unique angle $\beta = 97°$. The lattice constants were refined from neutron four-circle diffractometer data on 30 high-order reflections: $a = 5.3266(7)$, $b =$

0003–004X/80/0304–0349$02.00

Table 1. Atomic coordinates (as fractions of cell edges), neutron scattering lengths, population parameters, and anisotropic thermal parameters ($U_{ij} \times 10^{-2}$) of penninite. Standard deviation in the least significant figure(s) is in parentheses

Atom	b $[10^{-15}m]$	Popul.	x	y	z	U_{11}	U_{22}	U_{33}	U_{12}	U_{13}	U_{23}
$M_t(1)$	5.56(6)		.00	.00	.00	.38(13)	.51(11)	.94(11)	.15(7)	.08(7)	.06(7)
$M_t(2)$	5.56(5)		.0007(3)	.3336(1)	-.00004(9)	.61(9)	.52(7)	.69(7)	-.02(5)	.02(5)	-.03(5)
$M_b(1)$	5.11(5)		.0004(3)	.1667(1)	.5000(1)	.51(9)	.41(8)	1.22(8)	.01(5)	.16(5)	.09(5)
$M_b(2)$	4.89(6)		.00	.50	.50	.49(14)	.51(12)	1.04(13)	-.01(8)	.11(8)	-.04(8)
T(1)	3.95(4)		.2310(3)	.1672(2)	.1917(1)	.42(12)	.26(10)	.73(11)	.05(7)	.20(7)	.11(7)
T(2)	3.95(4)		.7314(3)	.0007(2)	.1917(1)	.44(12)	.19(11)	.72(11)	-.04(7)	.12(7)	-.11(6)
O(1)	5.8		.1932(2)	.1671(1)	.07697(8)	.53(7)	.58(6)	.64(6)	-.08(5)	.06(5)	-.03(4)
O(2)			.6922(2)	.0002(1)	.07689(8)	.59(7)	.61(6)	.66(7)	.01(5)	.15(5)	.03(5)
O(3)			.2120(3)	.3341(1)	.23254(9)	.91(6)	1.19(7)	.10(5)	.40(5)	-.01(5)	
O(4)			.5114(3)	.1003(1)	.23259(9)	1.43(8)	1.69(7)	1.10(7)	.38(6)	.08(5)	-.14(5)
O(5)			.0112(3)	.0676(1)	.23249(9)	1.35(8)	1.85(7)	1.07(7)	-.29(5)	.13(5)	.10(5)
O(6)		0.99(1)	.6914(2)	.3334(1)	.0730(2)	.73(9)	.61(7)	.64(15)	.15(5)	.11(6)	.04(5)
O(7)			.1465(3)	-.0002(1)	.4301(1)	1.64(8)	1.33(7)	.75(10)	.02(6)	.09(6)	.06(5)
O(8)			.1417(3)	.3346(1)	.4301(1)	1.70(8)	1.42(7)	.74(10)	.00(5)	.18(6)	-.06(5)
O(9)			.6413(2)	.1649(1)	.4303(1)	1.04(8)	1.47(7)	.90(10)	.07(5)	.01(6)	-.05(5)
H(1)	-3.74	0.93(2)	.7139(5)	.3339(3)	.1399(3)	3.60(20)	3.64(17)	.46(29)	.17(12)	-.02(11)	-.05(10)
H(2)		1.01(1)	.1193(5)	.0054(3)	.3632(2)	3.81(19)	3.84(16)	1.00(22)	-.14(12)	.34(11)	.02(11)
H(3)		1.00(1)	.1303(5)	.3353(3)	.3629(2)	4.30(20)	3.80(17)	1.15(23)	.00(12)	.10(11)	-.01(11)
H(4)		1.02(1)	.6143(5)	.1594(3)	.3635(2)	3.81(19)	3.83(16)	1.75(22)	.41(12)	.12(11)	-.11(11)

Table 2. Interatomic distances (A) and angles (°)

Atom	Distance	Atoms	Angle or Distance
T(1)-tetrahedron			
T(1)-O(1)*	1.639(2)		
-O(3)	1.657		
-O(4)	1.655		
-O(5)	1.653		
mean	1.651		
O(1)*-O(3)	2.711(2)	O(1)*-T(1)-O(3)	110.7(1)
O(1)*-O(4)	2.707	O(1)*-T(1)-O(4)	110.5
O(1)*-O(5)	2.709	O(1)*-T(1)-O(5)	110.8
O(3) -O(4)	2.683	O(3) -T(1)-O(4)	108.2
O(3) -O(5)	2.683	O(3) -T(1)-O(5)	108.3
O(4) -O(5)	2.682	O(4) -T(1)-O(5)	108.3
T(2)-tetrahedron			
T(2)-O(2)*	1.641(2)		
-O(3)'	1.654		
-O(4)	1.655		
-O(5)'	1.652		
mean	1.651		
O(2)+-O(3)'	2.707(2)	O(2)*-T(2)-O(4)	110.7(1)
O(2)+-O(4)	2.710	O(2)*-T(2)-O(5)	110.8
O(2)+-O(5)'	2.710	O(2)*-T(2)-O(3)'	110.5
O(3)'-O(4)	2.680	O(4) -T(2)-O(5)'	108.3
O(3)'-O(5)	2.681	O(4) -T(2)-O(3)'	108.2
O(4) -O(5)'	2.679	O(5)'-T(2)-O(3)'	108.4
octahedra			
$M_t(1)$-O(1)	2.094(1)x2	$M_t(2)$-O(1)	2.088(2)
-O(2)	2.090 x2		2.082
-O(6)	2.060 x2	-O(2)	2.090
			2.090
$M_b(1)$-O(7)	2.046(2)	-O(6)	2.062
	2.046		2.064
-O(8)	2.042		
	2.042	$M_b(2)$-O(7)	2.022(1)x2
-O(9)	2.046	-O(8)	2.026(2)x2
	2.046	-O(9)	2.020(2)x2

* indicates the apical oxygen in the tetrahedra

9.232(1), $c = 14.399(3)$A, $\alpha = 90°$, $\beta = 97.16(1)°$, $\gamma = 90°$ for a monoclinic cell. Microprobe analyses which were performed at three different positions of the investigated crystal gave the following average chemical components in weight percent: SiO_2: 32.8; Al_2O_3: 14.5; TiO_2: 0.009; FeO: 3.578; MgO: 34.6; MnO: 0.07 (CaO, Na_2O, K_2O, Cr_2O_3, CoO, NiO: 0.000). A calculation for 28 oxygens then yields the formula:

$$Mg_{9.80}Al_{1.64}Fe_{0.57}Mn_{0.01}(Si_{6.32}Al_{1.68})O_{20}(OH)_{16}$$

The OH content was not determined, but was refined in the least-squares calculations based on the scattering lengths of the hydrogen positions. The chemical formula indicates that this chlorite specimen is a penninite.

The intensity data were collected at room temperature on the D8 four-circle diffractometer at the Institute Laue-Langevin, Grenoble. The wavelength used was $\lambda = 1.2134$A from a Cu(200) monochromator. The flux at the sample position was 5×10^7n cm^{-2} sec^{-1} measured by gold foil activation. An $\omega/x\ \theta$ scan was applied according to the measured resolution curve. The intensities of about 1000 reflections were collected, resulting in a set of 856 unique intensities. In the refinement procedure only those with $|F_o|^2 > 2\sigma$ were included, altogether 725 reflections. An absorption correction ($\mu_{calc} = 0.95$ cm^{-1}) was applied by a Gaussian grid point method of $12 \times 12 \times 12$ points. For the refinement the program CRYLSQ of the X-RAY-SYSTEM (Stewart *et al.*, 1972)

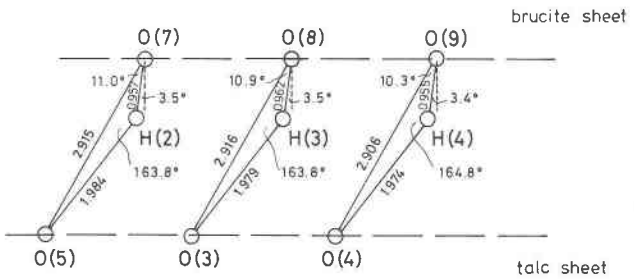

Fig. 1. Hydrogen-bond system between talc and brucite sheet.

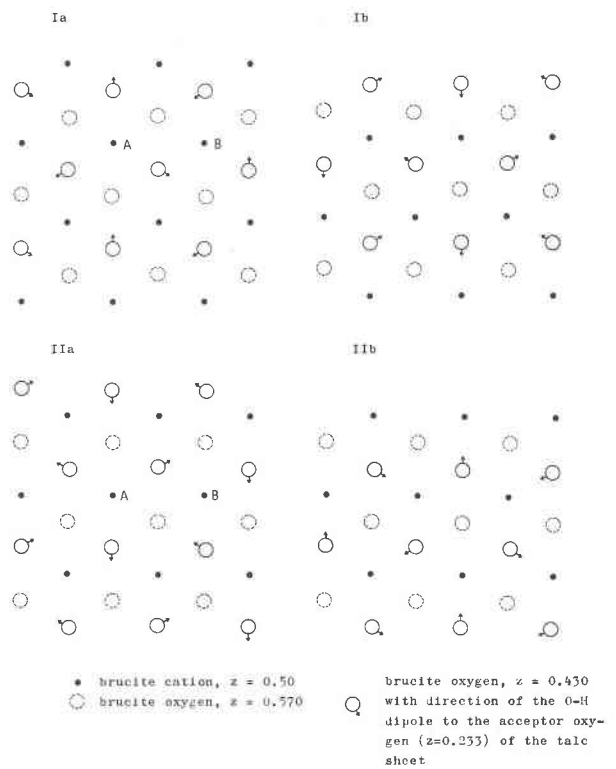

Fig. 2. Tilting modes of the O–H dipoles in direction to the acceptor oxygens of the talc sheet shown for the four chlorite layer types projected along z^*.

was used, and a weighting scheme with $w(F_0) = [\sigma_c^2 + 0.001\,F_0^2 + 5.0]^{-1}$ was employed. The following neutron scattering lengths were used (all given in units of 1 Fermi = 10^{-15}m): $b_{Si} = 4.2$, $b_{Al} = 3.5$, $b_{Mg} = 5.2$, $b_{Fe} = 9.5$, $b_O = 5.80$, $b_H = -3.74$ (Bacon, 1975). The refinement was carried out on positional parameters of all atoms, on the occupation numbers of the hydrogens, and the scattering lengths of the cation sites. Four unique structure types are possible for the space group $C\bar{1}$ and $C1$ with $\beta = 97°$, but the refinement converged only for the polytype II*b*-4 (or the equivalent type II*b*-6). Refinement in the asymmetric space group $C1$ for II*b*-4 was attempted but did not converge due to the limited number of observations, which led to high correlations. Moreover the $N(z)$ statistical test with reflections $k \neq 3n$ gave no clear answer on centrosymmetry. Space group $C\bar{1}$ was therefore adopted. Table 1 gives the final atomic parameters, and Table 2 the interatomic distances and angles.

Discussion

The structure consists of a talc network which, like the 1M phlogopite refined by neutron diffraction (Joswig, 1972), has an almost ideal hexagonal symmetry and brucite sheets of nearly trigonal symmetry. Marked distortions are only observed in the direction parallel to z^*. The tetrahedral sheet in the talc network is evenly expanded along z^*, whereas the octahedral one is contracted. The three pyramidal edges of the tetrahedra have mean lengths of 2.709(2)A for T(1) and 2.708(2)A for T(2). The mean lengths for the basal edges are 2.683(2) and 2.680(2)A respectively. The lateral dimension of the tetrahedral sheets is reduced by a rotation about the normal to the sheet to adjust the difference in dimension between the tetrahedral and octahedral network. This is a common feature in all mica structures and described by the O_b–O_b–O_b angle, which is =6.4° in this case. As the rotation axis is formed by the T–O_a bonding, both T–T–T as well as O_a–O_a–O_a angles are equal to 120°.

The two nonequivalent T sites show no cation or-

Table 3. Hydrogen-bonding scheme

O - H ... O	O - H	O ... O	H ... O	O - H...O	H - O...O
O(7)-H(2)...O(5)	.957(4)	2.915(2)	1.984(4)	163.8(3)	11.0(2)
O(8)-H(3)...O(3)	.962(4)	2.916(2)	1.979(4)	163.8(3)	10.9(2)
O(9)-H(4)...O(4)	.955(4)	2.906(2)	1.974(4)	164.8(3)	10.3(2)

dering, as revealed by the bond lengths as well as by the refinement of the scattering lengths. Likewise, no significant evidence was observed for cation ordering in the octahedral sites.

In the brucite sheet the existence of a partial cation ordering is significant because the refined scattering lengths are: b = 5.11(5) and 4.89(6) respectively for $M_b(1)$ and $M_b(2)$, and the mean bond lengths are: $M_b(1)$–O = 2.045(2)A and $M_b(2)$–O = 2.023(2)A. Ordering of Mg and Al was observed in the octahedral layers of the sheet silicate xanthophyllite (Takéuchi, 1965), but again no ordering in the silicate layer of this mica was detected.

Considering these differences in scattering lengths and in bond distances, we propose the following approximate ordering scheme in the brucite sheet: 2 × $(Mg_{1.75}Al_{0.25})$ at $M_b(1)$ and $(Mg_{1.5}Al_{0.5})$ at $M_b(2)$; the octahedral sites $M_t(1)$, $M_t(2)$ of the talc sheet are occupied by $(Mg_{4.8}Al_{0.6}Fe_{0.6})$. The partial substitution of Mg^{2+} by Al^{3+} in the brucite sheet causes it to acquire a positive charge, whereas the talc network has a negative net charge. This difference supplies an additional mechanism to the hydrogen-bond system for the interconnection of the sheets.

The hydrogen-bond system

The three symmetrically independent O–H dipoles are roughly perpendicular to the brucite sheet, but they are somewhat tilted towards the respective acceptor oxygen atoms of the silicate sheet. The deviation from 90° is 3.5(2)° for the H(2) and H(3) bridge and 3.4(2)° for H(4). The precise geometry is given in Figure 1 and Table 3. All hydrogen bonds formed between the sheets may be characterized as medium to weak according to the donor–acceptor distances.

The tilting modes of the O–H dipoles in forming hydrogen bonds give rise to a distortion of the electrostatic field from the tetrahedral configuration about each oxygen atom in the brucite sheet. Without the formation of hydrogen bonds the O–H dipoles would be perpendicular to the sheet, as observed in the brucite structure itself (Zigan and Rothbauer, 1967).

In general the tilting mode of the O–H dipoles in the various polytypes of chlorites can be classified into two groups with respect to the positions of the brucite cations (Fig. 2). The tilting modes for IIb and Ib are arranged in one category with the same tilting mode about every brucite cation. The modes for Ia and IIa form the other group. In this case the tilting mode with respect to each brucite cation is not identical. The mode about cation A is different from that of cation B (Fig. 1). We may therefore draw the conclusion that in IIb and Ib the electrostatic distortion in the brucite sheet is evenly distorted over the whole sheet, while in Ia and IIa the distortions are not identical. This even distribution in the polytypes Ib and IIb may be related to the fact that these two types occur more frequently in nature than Ia and IIa types. The differences in stability between IIb and Ib can be ascribed to the difference in cation repulsion (Shirozu and Bailey, 1965).

Acknowledgment

We are indebted to Dr. N. Haga, Mineralogical Institute, University of Tokyo, for performing the microprobe analyses. The calculations were carried out at the Hochschulrechenzentrum der Universität Frankfurt.

References

Bacon, G. E. (1975) *Neutron Diffraction, 3rd ed.* Oxford University Press, Oxford, England.

Bailey, S. W. and B. E. Brown (1962) Chlorite polytypism: I. Regular and semi-random one-layer structures. *Am. Mineral., 47,* 819–850.

Brown, B. E. and S. W. Bailey (1963) Chlorite polytypism: II. Crystal structure of a one-layer Cr-chlorite. *Am. Mineral., 48,* 42–61.

Joswig, W. (1972) Neutronenbeugungsmessungen an einem 1M-Phlogopit. *Neues Jahrb. Mineral. Monatsh.,* 1–11.

Shirozu, H. and S. W. Bailey (1965) Chlorite polytypism: III. Crystal structure of an orthohexagonal iron chlorite. *Am. Mineral., 50,* 868–885.

Steinfink, H. (1958) The crystal structure of chlorite. II. A triclinic polymorph. *Acta Crystallogr., 11,* 195–198.

Stewart, J. M., G. J. Kruger, H. L. Ammon, C. Dickinson and S. R. Hall (1972) *The XRAY system—version of June 1972.* Tech. Rep. TR-192, Computer Science Center, University of Maryland, College Park, Maryland.

Takéuchi, Y. (1965) Structures of brittle micas. *Clays and Clay Minerals, 13,* 1–25.

Zigan, F. and R. Rothbauer (1967) Neutronenbeugungsmessungen am Brucit. *Neues Jahrb. Mineral. Monatsh.,* 137–143.

Manuscript received, November 6, 1978;
accepted for publication, July 19, 1979.